

Kinetics and a Revised Mechanism for the Autocatalytic Oxidation of SCN^- by ClO_2

James N. Figlar and David M. Stanbury*

Department of Chemistry, Auburn University, Auburn, Alabama 36849

Received: April 8, 1999; In Final Form: June 1, 1999

The aqueous reaction of chlorine dioxide with excess thiocyanate is known to be autocatalytic at pH 2. We find that under strongly acidic conditions ($>0.1 \text{ M HClO}_4$) it is pseudo-first-order with respect to $[\text{ClO}_2]$. Under these conditions, the rate law is $-\text{d}[\text{ClO}_2]/\text{d}t = (2k_1 + 2k_2[\text{H}^+])[\text{ClO}_2][\text{SCN}^-]$, with $2k_1 = 0.42 \text{ M}^{-1} \text{ s}^{-1}$ and $2k_2 = 0.52 \text{ M}^{-2} \text{ s}^{-1}$ at 25°C and $\mu = 1 \text{ M}$ (LiClO_4). Effective activation parameters in 1 M HClO_4 are $\Delta H^\ddagger = 66.5 \text{ kJ/mol}$ and $\Delta S^\ddagger = -26.3 \text{ J/mol}$ for the temperature range $13.4\text{--}52.2^\circ\text{C}$. Reaction products were identified by ion chromatography and ion-selective electrodes, which allowed a verification of the stoichiometry, $6\text{ClO}_2 + 5\text{SCN}^- + 8\text{H}_2\text{O} \rightarrow 6\text{Cl}^- + 5\text{CN}^- + 5\text{SO}_4^{2-} + 16\text{H}^+$. Direct evidence for a reaction intermediate, thiocyanogen, was obtained through careful analysis of multiwavelength rapid scanning data. This intermediate provides a reactive autocatalytic species OSCN^- via hydrolysis equilibrium, and this equilibrium was found to be important to simulations and fits to raw data. A 14-step mechanism is employed for these fits and simulations, allowing a more thorough description of the reaction system; this mechanism successfully reproduces both the full rate law under pseudo-first-order conditions and the autocatalytic behavior at pH 2.

Introduction

The reaction of ClO_2^- with SCN^- has been of interest since 1985 when it was shown to display oscillations in a CSTR (continuously stirred tank reactor).¹ Subsequently, the reaction was shown to display chaos and to generate substantial amounts of ClO_2 as an intermediate.² ClO_2 has been confirmed as an intermediate in this reaction, and it has been used as a convenient spectrophotometric indicator of the oscillations in a CSTR and of the oligooscillations in batch.^{3,4} The participation of ClO_2 in the reaction is to be expected, since it occurs generally in the large family of chlorite oscillators.⁵ Understanding the reaction mechanisms of these systems would be an important step in extending the knowledge of this unusual and complex behavior. However, developing mechanisms to account for the production and loss of ClO_2 during these types of oscillations has been an ongoing problem due in large part to the complexity of chlorite oxidative chemistry.³

The chlorite/iodide system has been thoroughly examined,^{6,7} and although a mechanism has been proposed, it remains unclear as to the applicability of the empirical steps to other systems. In fact, a general model has been proposed that outlines a series of reactions thought to play a major role in chlorite oscillators.⁵ However, the authors do point out that for systems such as the $\text{ClO}_2^-/\text{I}^-$ system, where the oxidant plays a significant role in oscillations, this type of generalized model will likely not be universally applicable.⁵ Although originally viewed as perhaps the simplest chlorite–sulfur oscillating system to investigate mechanistically,¹ the chlorite/thiocyanate system has proved difficult in its own right.

Coupled to the difficulties arising from the oxidative chemistry of ClO_2^- are the inherent complexities associated with thiocyanate. The oxidized products of thiocyanate may undergo a variety of transformations including, but not limited to, dimerization, polymerization, disproportionation, and the formation of thiocyanogen.³ These complications have made the elucidation of a tractable mechanism for the oscillating reactions of the chlorite/thiocyanate system a difficult prospect.

One way to gain insight to this reaction mechanism is through a thorough examination of the reaction of chlorine dioxide and thiocyanate. Oscillations in this system can be avoided by limiting the concentration of chlorite produced to quantities dependent on the initial ClO_2 concentration.³ However, autocatalysis is noted at relatively low pH's.³ Despite this type of behavior, a mechanism has been proposed for this reaction and was used to support specific assertions related to the $\text{ClO}_2^-/\text{SCN}^-$ oscillators.³ The 21-step mechanism invoked HOCl and Cl^- as autocatalytic species for the reaction.³ Careful examination of this work reveals a number of problems with this proposed reaction pathway. The more obvious errors in this mechanism include chloride as an autocatalytic species,⁸ a mechanism that is inconsistent with the simulation results,⁸ and the omission of known reaction paths related to this system.

We report in this paper a re-evaluation of the mechanism for the reaction of ClO_2 with thiocyanate through a careful examination of the reaction kinetics via multiwavelength rapid scanning techniques, mathematical simulations, and significant alterations to the reaction conditions which afford pseudo-first-order behavior. The results of this work have afforded the deduction of what we feel to be a more representative mechanism. The elementary reactions depicted in the 14-step mechanism are, in nearly all cases, drawn from what is known or has been reported in the literature. Similarly, the rate constants used to simulate and fit the data are also drawn directly or kept within reasonable ranges of the values noted in the literature.

Experimental Section

Reagents. The following were purchased from JT Baker and used without further purification: $\text{K}_2\text{S}_2\text{O}_8$, boric acid, LiOH , and KHP . NaSCN (Baker) was recrystallized from water. The following reagent grade materials were purchased from Fisher and used without further purification: phenol, acetonitrile, NaCN , and sulfuric (96%) and perchloric acids (75%). $\text{NaClO}_4 \cdot \text{H}_2\text{O}$ (Fisher) was recrystallized from hot water prior to use. 1,10-Phenanthroline was purchased from Aldrich and used

without further purification. 5,5-Dimethyl-1-pyrroline-*N*-oxide (Aldrich) was vacuum distilled prior to use. NaClO₂ (anhydrous) was purchased from Kodak and was recrystallized from hot water prior to use. LiClO₄ was prepared by the metathesis of LiOH and HClO₄ and recrystallized from hot water. Tridodecylmethylammonium chloride, PVC, and THF (>99.5%) were purchased from Fluka and used without further purification. Distilled deionized water was used throughout.

Synthesis of ClO₂. Aqueous solutions of ClO₂ were prepared with a few alterations to the method described previously.⁹ In a three-neck flask, a 5 g (55 mmol) sample of NaClO₂ was dissolved with approximately 10 mL of deionized distilled water. A solution of 1.5 g (5.5 mmol) of K₂S₂O₈ in approximately 50 mL of water was added dropwise to the NaClO₂ solution. For 2 h, a stream of N₂(g) was bubbled through the yellow reaction mixture, which forced the product gas through a tube containing NaClO₂ powder. The gas stream was then bubbled into approximately 150 mL of water buffered at pH 2.0 with perchloric acid contained in a brown bottle. This reaction was run in the dark at all times and behind an explosion shield. All ClO₂ solutions were stored in a brown bottle and kept in a refrigerator.

Analytical Methods. The concentrations of ClO₂ were determined spectrophotometrically with an HP 8453 spectrophotometer; determinations used for ClO₂ $\epsilon_{360} = 1200 \text{ M}^{-1} \text{ cm}^{-1}$.¹⁰ Thiocyanate solutions were titrated iodometrically with standardized thiosulfate solutions, and the average purity was found to be >95%. All pH measurements were performed on a Corning model 130 pH meter, using either a standard Corning combination pH electrode or a Mettler combination pH electrode.

Ion Chromatography. Reaction product determinations were made using a Wescan ion analyzer, model 266. The instrument was fitted with a 100 μL sample loop, a Wescan Versapump-II and model 213A electrical conductivity and model 271 electrochemical detectors. The electrochemical (amperometric) detector utilized a Pt working electrode, a Pt auxiliary electrode, and a Ag/AgCl reference electrode. A 25 cm resin-based anion exchange column (Wescan anion/R) and 2.0–4.0 mL flow rates were employed depending on the eluent and ions detected. Results were recorded on a strip-chart recorder. Eluents used for these determinations were 4 mM KHP (eluent 1) and 0.3 mM KHP/1 mM boric acid/10% acetonitrile at pH 11.9 (eluent 2). Product concentrations were determined by peak height analysis from calibration curves of standard solutions. The concentration of CN⁻, as a product of the reaction of ClO₂ with SCN⁻, was determined by treating product solutions with 1 M KOH prior to analysis to remove excess perchlorate present in the solution. After treatment, the solutions were analyzed with eluent 1. Five replicate experiments showed CN⁻ ion to be present at a concentration of $0.58 \pm 0.12 \text{ mM}$ for initial reactant concentrations of 0.5 mM ClO₂ and 5.0 mM SCN⁻. Chloride ion was determined by ion chromatography with eluent 2, the reaction solutions containing either of two acids (HClO₄ and H₂SO₄) at identical starting concentrations of ClO₂ (0.5 mM) and SCN⁻ (2.5 mM). Product solutions containing HClO₄ were treated with KOH to precipitate excess ClO₄⁻, and solutions containing H₂SO₄ were treated with Ba(OH)₂ to pH 7.0 in order to precipitate excess SO₄²⁻. Both methods produced average Cl⁻ concentrations of $0.578 \pm 0.041 \text{ mM}$ from sets of three replicate samples. Residual SCN⁻ concentrations were determined similarly, utilizing 1 M H₂SO₄ solutions. Product analysis reflected an average [SCN⁻] loss of $0.58 \pm 0.10 \text{ mM}$ from five replicate samples. Product analysis could only provide qualitative identification of SO₄²⁻ as a reaction product. A variety of additional standard calibration curves were determined

for the following ions, although none were detected in the reaction mixture: ClO₃⁻, ClO₄⁻, ClO₂⁻, and OCN⁻. All \pm errors represent the standard deviation of replicate experiments.

Potentiometric Determinations. The yield of Cl⁻ plus CN⁻ and their evolution over time were also measured by use of a Cl⁻ selective electrode. The electrode was constructed by casting a PVC film containing a Cl⁻-selective ionophore in a glovebox supplied by nitrogen and mounting this membrane to a standard electrode body using a 10 mM Cl⁻ solution as an electrolyte. The electrode membrane was cast according to the manufacturer's specifications (Fluka) for the ionophore tridodecylmethylammonium chloride. This type of membrane is of the classical solid-state variety, whereby the selectivity is a function of the stability products for the individual complexes.¹¹ Thus, selectivity coefficients can be derived for a variety of possible interferences as shown by the manufacturer.¹² Membranes were fabricated from an 80/20 by weight ionophore/PVC mixture. The mixture was dissolved in THF and then allowed to evaporate for casting.¹² Excellent film thicknesses were achieved by using a total weight of $\sim 1.5 \text{ mg}$ of the ionophore/PVC solid and dissolved by vigorously shaking in a capped vial with $\sim 1.5 \text{ mL}$ of solvent. Potentials were measured against a standard calomel reference, with a Corning model 130 pH meter set to the mV functionality.

This electrode membrane shows little selectivity for SO₄²⁻, and thus reactions were monitored in 1 M sulfuric acid. The electrode was calibrated by standard additions of NaCl solutions. The membrane did show selectivity for CN⁻ by the same calibration methods. This allowed for the evaluation of CN⁻ evolution as well as Cl⁻; however, this evaluation is represented by collective potential differences. These potential differences were monitored ~ 4 –6 min after initiation of the reaction, which coincides with approximately 99% completion for the reaction conditions, 50 mM SCN⁻ and 5.8 mM ClO₂ initial concentrations. Calibration curves for Cl⁻ and CN⁻ were constructed in the presence of 50 mM SCN⁻ and 1 M H₂SO₄ and had slopes of 0.26 and 0.48 mV/mM, respectively, in the region of 15 mM substrate.

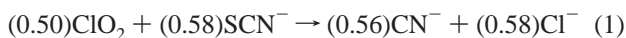
Kinetic Methods. Initial kinetic measurements were conducted on a Hi-Tech Scientific stopped-flow apparatus, model SF-51, equipped with an SU-40 spectrophotometer unit in the 1.0 cm path length configuration. The temperature was maintained at 25 °C with a C-400 circulating water bath, except when conducting the temperature dependence study, whereby the temperature was maintained at varying values within the range of 13.4–52.2 °C. The absorbance decrease at 360 nm was monitored by mixing equal volumes of ClO₂ and SCN⁻ solutions at varied concentrations. The output from the SU-40 unit was collected by an On-line Instruments (OLIS) 4300 data acquisition system based on a Zenith computer. The pseudo-first-order rate constants were evaluated by exponential fits with the OLIS subroutines. Multiwavelength experiments were performed using the OLIS rapid scanning monochromator stopped-flow system (RSM 1000) with the USA-SF mixing attachment (1.7 cm path length). Data were acquired and processed with dual-beam UV–vis recording and a global fitting subroutine. Spectral changes were monitored in the UV–vis region (275–400 nm) and analyzed additionally by using the Specfit software package.¹³ Kinetic simulations were also performed by utilizing the Specfit package.

Results

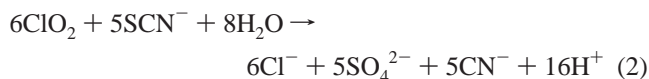
Initial attempts at studying the mechanistic parameters of the ClO₂/thiocyanate reaction system afforded some difficulties. The

characteristic absorbance decay profile of ClO_2 at 360 nm was noted to be autocatalytic at reasonable ClO_2 concentrations in the presence of excess SCN^- at pH 2.0. A number of spin traps were utilized to determine if free radical formation was responsible for the autocatalytic behavior. Increasing concentrations of PBN, DMPO, and phenol added to the reaction mixture at pH 2.0 increased the overall time course of the reaction and reduced the degree of autocatalysis, but limiting pseudo-first-order behavior was not attained even at the highest concentrations of these scavengers. However, pseudo-first-order behavior was found to occur at high acid concentrations ($\sim 1 \text{ M H}^+$) in the absence of spin traps. Thus, by examining these reactions under conditions of high acidity, a variety of mechanistic parameters were determined.

Stoichiometry. The stoichiometry of the reaction of ClO_2 with SCN^- in 1 M acid was examined by ion chromatography. Ion chromatography experiments were conducted on solutions of 1 mM initial ClO_2 and 5 or 10 mM SCN^- adjusted to 1 M acid with either HClO_4 or H_2SO_4 by mixing 10 mL of the ClO_2 solution with 10 mL of the thiocyanate solution in a stoppered 100 mL three-neck flask and allowing the reaction to proceed for at least 30 min in the dark at room temperature. The resultant product solution was then treated either with $\text{Ba}(\text{OH})_2$ (for H_2SO_4 solutions) or KOH (for HClO_4 solutions) prior to analysis. Anionic products were determined to be CN^- , Cl^- , SCN^- , and SO_4^{2-} . Quantitation by peak height analysis with standard calibration curves was achieved for CN^- , Cl^- , and SCN^- ions, but SO_4^{2-} could only be identified qualitatively. The analysis of SCN^- consumption and product yields relative to ClO_2 gave the following results:



Thus, by balancing for redox equivalents and assuming the mass balance for S is converted to SO_4^{2-} as noted qualitatively, the stoichiometry for this reaction appears to be



Additional support for the stoichiometry in eq 2 is found from the results of the ion-selective electrode experiments. Over the course of three replicate experiments, an average potential change of 3.4 mV was noted for the reaction of 5.8 mM ClO_2 with 50 mM SCN^- over approximately a 4–6 min period at pH 0.0. Based on the Cl^- calibrations and a starting concentration of ClO_2 (5.8 mM), a 100% conversion to Cl^- would result in a 1.5 mV change. The yield of CN^- , based on a ClO_2/CN^- ratio of 6:5, would contribute an additional 2.3 mV change, for a total expected potential change of 3.8 mV. In view of the small potential changes involved, the agreement is satisfactory and supports the yields of Cl^- and CN^- obtained in the ion chromatography experiments; moreover, these potentiometric results indicate that these products are formed on a time scale comparable to the kinetics of the reaction as described below.

Similar reaction stoichiometries and product formations are reported for the reactions of chlorite/thiourea^{14,15} and chlorite/thiocyanate;¹ however, Chinake et al. report qualitative evidence that CN^- is not present in the product solution of the chlorite/thiocyanate reaction, and they infer the formation of OCN^- from measurements of consumption ratios.³ Similarly, from a consumption ratio of 8:5 for $\Delta\text{ClO}_2/\Delta\text{SCN}^-$, they infer cyanide instead of cyanide in the direct reaction of chlorine dioxide and

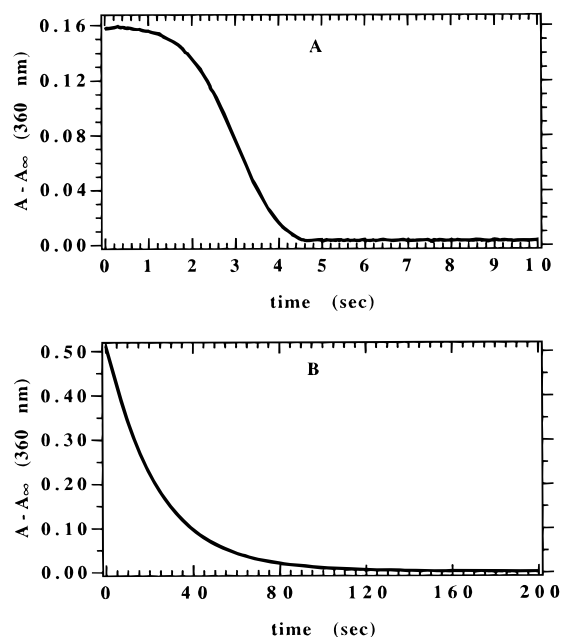


Figure 1. ClO_2 absorbance decay profiles at pH 2.0 and 0.0. The kinetic data were taken on a Hi-Tech Scientific Stopped Flow. (A) Decay plot of $(A - A_\infty)$ at 360 nm as a function of time for the reaction of ClO_2 with excess SCN^- in pH 2.0 perchlorate buffer at 25 °C. $[\text{ClO}_2]_0 = 0.13 \text{ mM}$ and $[\text{SCN}^-] = 25 \text{ mM}$. (B) Decay plot of $(A - A_\infty)$ at 360 nm as a function of time for the reaction of ClO_2 with excess SCN^- in 1 M perchloric acid at 25 °C. $[\text{ClO}_2]_0 = 0.50 \text{ mM}$ and $[\text{SCN}^-] = 50 \text{ mM}$.

thiocyanate.³ It is difficult to explain the difference between these results and ours, because the pH in the experiments of Chinake et al. was not specified, but one possibility is that the experiments of Chinake et al. were performed with excess ClO_2 , which could lead to the conversion of CN^- to OCN^- . Thus, the stoichiometry as in eq 2 is appropriate under the conditions of our kinetics studies.

Kinetics. The kinetics of the loss of ClO_2 with excess SCN^- at pH 2.0 at 25 °C shows significant deviations from pseudo-first-order behavior as shown in Figure 1a and is best described as autocatalytic. This behavior is fully in agreement with prior observations.³ Under these conditions, the reaction comes to completion in less than 10 s depending on the initial concentrations.

Under conditions of high acid concentration ($>0.1 \text{ M}$), the kinetic behavior changes drastically, becoming pseudo-first-order, as shown in Figure 1b. The time for complete ClO_2 consumption at high acid concentration significantly increases from less than 10 s (at pH 2.0) to greater than 100 s depending on the initial conditions. In blank tests, it was noted that in the absence of SCN^- but otherwise under the same conditions or with 0.01 M Cl^- that the loss of ClO_2 occurs on a much longer time scale. This demonstrates that the decay profiles in the presence of SCN^- do not correspond to ClO_2 disproportionation or Cl^- interactions due to contamination, which had been suggested as a catalytic species by others.³ In fact, appreciable interactions between Cl^- and ClO_2 are unlikely, as shown by earlier tracer studies^{16,17} and the early work of Bray¹⁸ as well as direct measurements and calculations performed in this laboratory.⁸ The acid-dependent behavior of the $\text{SCN}^-/\text{ClO}_2$ reaction thus reflects the intrinsic behavior of the system.

This drastic transition from autocatalytic to pseudo-first-order behavior can be expressed quantitatively by comparing the ratio of first and second half-lives as a function of acid concentration,

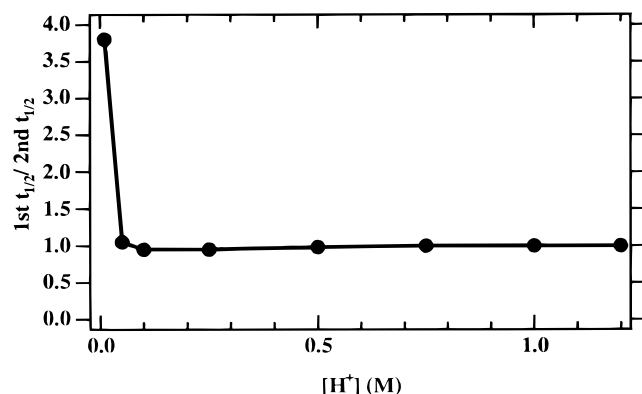


Figure 2. The effect on the ratio of the first and second half-times of the reaction of ClO₂ and SCN⁻ as a function of acid concentration. Solid line is a smooth curve to guide the eye. The kinetic data were taken on the Hi-Tech Scientific Stopped Flow at 360 nm at 25 °C in 1 M HClO₄; [ClO₂]₀ = 0.5 mM, [SCN⁻]₀ = 50 mM.

Figure 2. The ratio remains very close to 1 as the acid concentration drops, until the acid concentration reaches approximately 0.05 M, at which point greater deviations from 1 are noted. Although a thorough examination of the acid dependence between 0.05 and 0.01 M was not attempted, it seems likely that a steady progression in this ratio proceeds until, at 0.01 M, the ratio becomes nearly 4.0.

It has been shown that the generation and decay of ClO₂ in the batch reaction of ClO₂⁻ with SCN⁻ at pH 2 is mildly affected by the presence of trace levels (10 μM) of Cu²⁺.⁴ Accordingly, we have conducted experiments to test for the effects of Cu²⁺ on the direct reaction of ClO₂ with SCN⁻. These experiments were performed by examining the effect of phenanthroline as an additive that would chelate adventitious metal ions, a method that has been used in controlling metal ion catalysis in the reaction of [IrCl₆]²⁻ with thiourea.¹⁹ We find that the presence of 50 μM phenanthroline has no effect on the loss of ClO₂ for reactions conducted at pH 2 with 50 mM SCN⁻ and 0.3 mM ClO₂. This result demonstrates that the other results described in this paper are not affected by the presence of adventitious metal ions.

The consumption of ClO₂ under strongly acidic (pseudo-first-order) conditions follows the rate law

$$-d[\text{ClO}_2]/dt = k_{\text{obs}}[\text{ClO}_2] \quad (3)$$

The values of k_{obs} are sensitive to the concentrations of SCN⁻ and H⁺ and are summarized in Table 1. As shown in Figure 1S of the Supporting Information, the plot of k_{obs} versus [SCN⁻] in 1 M acid is linear with an intercept near zero, which indicates that the rate law is first order with respect to [SCN⁻] under these conditions. Working within the range of pseudo-first-order behavior, ~0.25 to 1 M acid, as shown in Figure 2S of the Supporting Information, the plot of k_{obs} vs [H⁺] at 50 mM SCN⁻ is linear with an apparent nonzero extrapolated intercept, indicating a two-term rate law. Experiments at a variety of thiocyanate concentrations show that both terms are first order in [SCN⁻], as represented by

$$k_{\text{obs}} = 2k_1[\text{SCN}^-] + 2k_2[\text{SCN}^-][\text{H}^+] \quad (4)$$

A thorough examination of all the collected data was obtained through the use of a Gauss–Newton nonlinear least-squares fitting routine.²⁰ The fitting routine converged on a solution with values for $2k_1$ and $2k_2$ of $0.42 \pm 0.07 \text{ M}^{-1} \text{ s}^{-1}$ and 0.52 ± 0.09

TABLE 1: Kinetic Data for the Reaction of ClO₂ with SCN⁻ in High Acid Concentrations^a

$10^2 \times k_{\text{obs}}, \text{ s}^{-1b}$	replicates	[ClO ₂] ₀ , mM	[SCN ⁻], M	[H ⁺], M
25.1(1)	5	0.25	2.50×10^{-1}	0.5
12.5(2)	5	0.25	1.50×10^{-1}	0.5
7.82(25)	5	0.25	1.00×10^{-1}	0.5
1.82(3)	5	0.25	2.50×10^{-2}	0.5
28.4(3)	5	0.25	2.50×10^{-1}	1.0
12.5(3)	5	0.25	1.50×10^{-1}	1.0
10.2(4)	10	0.25	1.00×10^{-1}	1.0
4.54(48)	10	0.25	5.00×10^{-2}	1.0
2.14(6)	10	0.25	2.50×10^{-2}	1.0
1.18(1)	10	0.25	1.25×10^{-2}	1.0
0.407(33)	4	0.25	2.50×10^{-3}	1.0
0.431(21) ^c	5	0.25	2.50×10^{-3}	1.0
7.66(50)	5	0.50	5.00×10^{-2}	1.2
4.35(20)	5	0.50	5.00×10^{-2}	1.0
3.70(2)	5	0.50	5.00×10^{-2}	0.9
4.03(4)	5	0.50	5.00×10^{-2}	0.75
3.29(3)	5	0.50	5.00×10^{-2}	0.50
2.52(2)	5	0.50	5.00×10^{-2}	0.25
5.18(10)	5	0.22	5.00×10^{-2}	1.0
5.07(6)	5	0.32	5.00×10^{-2}	1.0
4.62(7)	5	0.85	5.00×10^{-2}	1.0
4.98(20)	5	0.65	5.00×10^{-2}	1.0

^a 25.0 °C, $\mu = 1.0 \text{ M}$ (LiClO₄) or in 1 M HClO₄. ^b Measured as the consumption of ClO₂ at 360 nm. Parenthetical values represent the error as three standard deviations. ^c Experiments were performed in 1 M H₂SO₄.

M⁻² s⁻¹, respectively. The rate law for the overall process in sufficiently acidic media is

$$-d[\text{ClO}_2]/dt = 2k_1[\text{ClO}_2][\text{SCN}^-] + 2k_2[\text{ClO}_2][\text{SCN}^-][\text{H}^+] \quad (5)$$

Composite activation parameters were determined from the temperature dependence of the rates in 1 M perchloric acid. These parameters were obtained by plotting $\ln\{k_{\text{obs}}/([\text{SCN}^-]T)\}$ vs $1/T$ and thus do not account for the acid dependence. These results are illustrated by the Eyring plot in Figure 3S of the Supporting Information, which yields values of $\Delta H^\ddagger = 66.5 \text{ kJ/mol}$ and $\Delta S^\ddagger = -26.3 \text{ J K}^{-1} \text{ mol}^{-1}$.

An interesting feature of rate law 5 is the lack of a term second order in [SCN⁻]. Such overall third-order terms are widely encountered for reactions of SCN⁻ with one-electron oxidants.^{21,22} A relevant comparison can be made with the reaction of [Ni(tacn)₂]³⁺, which has virtually the same self-exchange rate constant and E° value as ClO₂.²¹ For [Ni(tacn)₂]³⁺, the third-order rate constant is $2.0 \text{ M}^{-2} \text{ s}^{-1}$; because of electrostatic considerations, the corresponding rate constant for ClO₂ might be expected to be a factor of 10 less. A simple calculation shows that this factor of 10 is sufficient to give a third-order term that contributes negligibly to the ClO₂/SCN⁻ reaction under our conditions.

Detection of an Intermediate in 1 M H⁺. An important observation was noted when this reaction was studied in 1 M acid at multiple wavelengths when using rapid scan spectrophotometry. As shown in Figure 3, the absorbance profiles within the range 265–406 nm demonstrate nonisobestic behavior, indicative of complex kinetics. Extracting single-wavelength absorbance plots within the 265–300 nm range produced traces that show rise–fall behavior, characteristic of a short-lived intermediate; see Figure 4.

Another method by which the presence of an intermediate may be recognized is evolving factor analysis (EFA). This method uses a matrix algebraic treatment of the multiwavelength

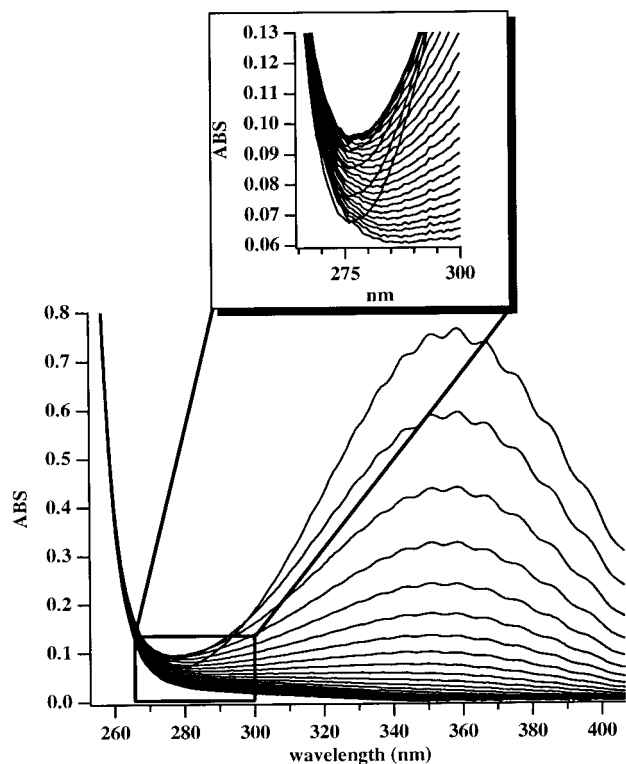


Figure 3. Multiwavelength decay profile of the reaction of ClO_2 and SCN^- . The multiwavelength kinetic data were taken on the RSM 1000 at 25 °C in 1 M HClO_4 ; $[\text{ClO}_2]_0 = 0.37 \text{ mM}$, $[\text{SCN}^-]_0 = 25 \text{ mM}$. The full scan depicts spectra sparsed at 5.95 s intervals. The enhanced area (boxed) between 265 and 300 nm for clarity shows only the first 100 s of the reaction at 3.96 s intervals, indicating that the reaction does not pass through an isosbestic point.

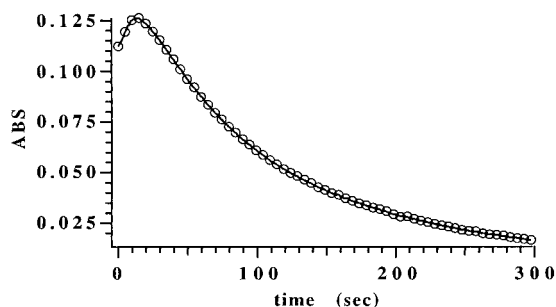


Figure 4. Absorbance changes at 275 nm for the reaction of ClO_2 and SCN^- . The multiwavelength kinetic data were taken on the RSM 1000 at 25 °C in 1 M HClO_4 ; $[\text{ClO}_2]_0 = 0.5 \text{ mM}$, $[\text{SCN}^-]_0 = 25 \text{ mM}$. The solid line represents the connectivity of all data points at 275 nm in the time profile; the open circles represent data points sparsed at five point intervals.

data to deduce the significant multidimensional minima in a data set which correspond to the probable number of significant species for that set.^{23–26} This type of treatment, available with the Specfit program, allows for “model-free” data transformation and yields qualitative information regarding both species concentration and spectral profiles.^{23–26} Because this method is a completely abstract interpretation of the spectrophotometric data, “sound chemical reasoning” is a prerequisite when interpreting the results.²⁵

Figure 5 presents the spectra resulting from a three-component EFA analysis of a multiwavelength data set for a reaction conducted in 1 M H^+ . The analysis was performed in the ABS mode, which normalizes the spectra to their maxima in the spectral range observed. The figure shows that this method is successful in identifying the spectral profile of ClO_2 (A) and

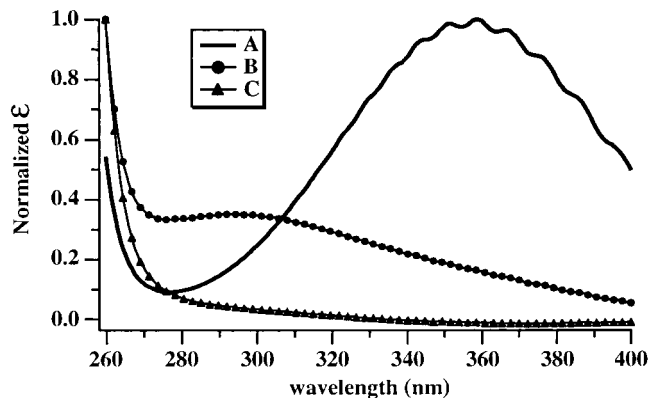


Figure 5. Spectral traces generated by EFA (ABS mode). The multiwavelength kinetic data were taken on the RSM 1000 at 25 °C in 1 M HClO_4 ; $[\text{ClO}_2]_0 = 0.45 \text{ mM}$, $[\text{SCN}^-]_0 = 25 \text{ mM}$. System is constrained to three components: component A (solid line) correlates well with the ClO_2 spectrum; component B (circles) is the intermediate $(\text{SCN})_2$; component C (triangles) reflects the contributions from the final products Cl^- , SO_4^{2-} , and CN^- .

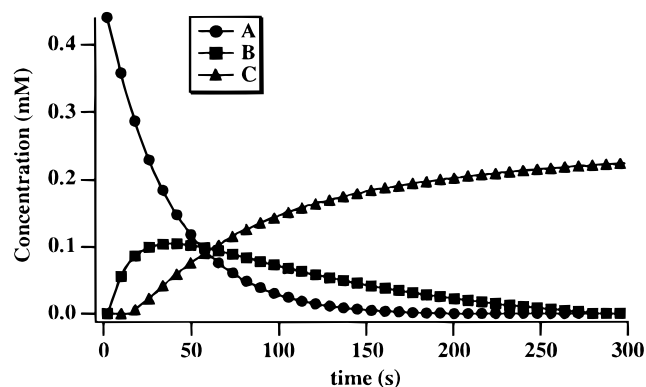


Figure 6. Concentration profiles for components A, B, and C as determined by EFA (ABS mode). For species B and C, the concentrations are scaled according to their normalized spectra. The multiwavelength kinetic data were taken on the RSM 1000 at 25 °C in 1 M HClO_4 ; $[\text{ClO}_2]_0 = 0.45 \text{ mM}$, $[\text{SCN}^-]_0 = 25 \text{ mM}$. System is constrained to three components: profile A (circles) is identical to the decay profile of ClO_2 at 360 nm; profile B (squares) is similar to the single wavelength profile of the raw data at 275 nm; profile C (triangles) is similar to the evolution of Cl^-/CN^- by ion selective electrode.

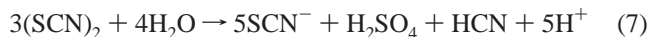
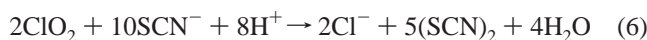
predicts the spectral profiles of intermediate B and final products C. The UV spectrum of species B is broad and has λ_{max} around 275 nm. Figure 6 displays the concentration profiles generated by EFA analysis. These concentration profiles reflect changes in each component relative to the changes of the initial absorbing species (ClO_2), as modulated by the normalized spectra in Figure 5. Therefore, the “concentrations” indicated for species B and C are related to their true concentrations by the ratio of the true and normalized molar absorptivities. Without further information, these data should be interpreted from a strictly qualitative viewpoint. Nonetheless, the concentration profiles accurately reflect the loss of ClO_2 determined independently, present convincing evidence for the formation and loss of an intermediate as implied by the single-wavelength data at 275 nm (Figure 4), and show product formation that is similar to the Cl^-/CN^- evolution, as seen with the ion-selective electrode.

These results show that a detectable short-lived intermediate is evolved during the course of the reaction under conditions of high acidity. We suggest that this intermediate is $(\text{SCN})_2$, which can be prepared as a stable solution in CCl_4 and has a UV spectrum with λ_{max} at 295 nm in that solvent.²⁷ In view of

TABLE 2: Mechanism for the Reaction of Chlorine Dioxide and Thiocyanate

no.	reaction		rate constant
SR1	ClO ₂ + SCN ⁻ → ClO ₂ ⁻ + SCN	<i>k</i> ₁	2.1 × 10 ⁻¹ M ⁻¹ s ⁻¹
SR2	H ⁺ + ClO ₂ + SCN ⁻ → HClO ₂ + SCN	<i>k</i> ₂	2.6 × 10 ⁻¹ M ⁻² s ⁻¹
SR3	SCN + SCN ⁻ → (SCN) ₂ ⁻		9 × 10 ⁹ M ⁻¹ s ⁻¹
SR4	(SCN) ₂ ⁻ + ClO ₂ → (SCN) ₂ + ClO ₂ ⁻		9 × 10 ⁹ M ⁻¹ s ⁻¹
SR5	(SCN) ₂ + H ₂ O ⇌ HOSCN + SCN ⁻ + H ⁺	<i>K</i> _{hyd}	4.4 × 10 ³ s ⁻¹ , 5 × 10 ⁵ M ⁻² s ⁻¹
SR6	HClO ₂ ⇌ H ⁺ + ClO ₂ ⁻	<i>K</i> _{a,Cl(V)}	1.9 × 10 ⁸ s ⁻¹ , 1 × 10 ¹⁰ M ⁻¹ s ⁻¹
SR7	HOSCN ⇌ H ⁺ + OSCN ⁻	<i>K</i> _{a,HOSCN}	5.01 × 10 ⁴ s ⁻¹ , 1 × 10 ¹⁰ M ⁻¹ s ⁻¹
SR8	HClO ₂ + SCN ⁻ → OSCN ⁻ + HOCl		180 M ⁻¹ s ⁻¹
SR9	HOCl + SCN ⁻ → [ClSCN] → HOSCN + Cl ⁻		1 × 10 ⁷ M ⁻¹ s ⁻¹
SR10	ClO ₂ + OSCN ⁻ → ClO ₂ ⁻ + OSCN		4 × 10 ⁶ M ⁻¹ s ⁻¹
SR11	2OSCN $\xrightarrow{H_2O}$ HO ₂ SCN + HOSCN		1 × 10 ⁷ M ⁻¹ s ⁻¹
SR12	2HO ₂ SCN → HOSCN + HO ₃ SCN		2 × 10 ⁸ M ⁻¹ s ⁻¹
SR13	2HOSCN → HO ₂ SCN + SCN ⁻ + H ⁺	<i>k</i> _{disp}	8 × 10 ² M ⁻¹ s ⁻¹
SR14	H ₂ O + HO ₃ SCN → H ₂ SO ₄ + HCN		5 × 10 ⁸ s ⁻¹

likely solvent effects, this spectral feature is in reasonable agreement with the EFA spectrum of intermediate B. Further support for identification of this intermediate as (SCN)₂ comes from the EFA analysis of its decay kinetics. Thiocyanogen is known to be unstable in aqueous solution, decaying in acidic media to give SCN⁻, HCN, and SO₄²⁻; it decays on the same time scale as indicated for the EFA decay of intermediate B.^{28,29} These suggestions are summarized by the following two-stage scheme for the overall reaction in 1 M H⁺:



As is shown below, in less acidic media steps occur that break down this neat two-stage description.

Discussion

Table 2 presents a 14-step mechanism that accounts for our observations and is consistent with well-established chemistry. It differs from the mechanism proposed by Chinake et al.³ both in the character of several of the steps proposed as well as in the magnitude of the rate constants for steps that are common to both mechanisms. The differences between the two mechanisms have arisen because of the demands imposed by our new data as well as a critical evaluation of the supporting literature. In what follows, we give a qualitative description of the mechanism, demonstrate the agreement between the predictions of the model and the observed data, and discuss details of the rate constants involved.

Qualitative Features of the Mechanism. Conceptually, the mechanism in Table 2 consists of three groups of reactions. The first set comprises steps SR1 through SR9; this nine-step group is sufficient to describe the conversion of ClO₂ and SCN⁻ to Cl⁻ and (SCN)₂ in 1 M H⁺ as in reaction 6. The second set, steps SR12 through SR14, are added to account for the decomposition of (SCN)₂ to HCN and SO₄²⁻, as in reaction 7. The third set, steps SR10 and SR11, becomes significant only at higher pH and is essential in generating the autocatalytic behavior seen at pH 2.

In 1 M H⁺, the species OSCN⁻ is largely converted to HOSCN (p*K*_a = 5.3),³⁰ so steps SR10 and SR11 can be neglected. The remaining steps with the rate constants indicated lead to the observed pseudo-first-order consumption of ClO₂, as in rate law 5. Moreover, the formation of (SCN)₂ occurs coherently with the consumption of ClO₂, as indicated in reaction 6, because the interconversion of (SCN)₂ and HOSCN via SR5 is rapid. Decomposition of (SCN)₂ as in reaction 7 is slow in 1 M H⁺ because it occurs through the rate-limiting second-order self-

reaction of HOSCN (SR13), the concentration of which is low because of its reversible conversion to (SCN)₂ (SR5).

One particularly troubling aspect of this chemistry pertains to the conflicting literature reports relating to the decomposition of (SCN)₂. Some facts are clear. (1) (SCN)₂ can be prepared as a reasonably stable solution in solvents such as CCl₄. (2) (SCN)₂ decomposes in acidic aqueous solution as in reaction 7. (3) The decomposition of (SCN)₂ in alkaline media yields OSCN⁻ as a stable species. There seems to be good evidence^{28,29} that the decomposition in acidic media obeys a second-order rate law as in

$$-\frac{d[(\text{SCN})_2]}{dt} = \frac{k_{\text{dec}}[(\text{SCN})_2]^2}{[\text{H}^+][\text{SCN}^-]^2} \quad (8)$$

The rate constant at 0 °C and μ = 1 M was reported to be 1 × 10⁻³ M³ s⁻¹.²⁹ The inferred mechanism entails the reversible hydrolysis of (SCN)₂ to HOSCN as in SR5 (*K*_{hyd}) followed by the second-order self-reaction of HOSCN as in SR13 (*k*_{disp}). Some support for the proposed formation of HO₂SCN in SR13 is provided by the recent report of the synthesis of a salt of O₂SCN⁻.³¹ Rapid follow-up steps SR12 and SR14 lead to the conversion to final products, as suggested in Table 2. If the steady-state approximation is made for HO₂SCN when pH ≪ p*K*_{a,HOSCN}, reactions SR5 and SR12 through SR14 lead to the rate law

$$-\frac{d[(\text{SCN})_2]}{dt} = \frac{3k_{\text{disp}}(K_{\text{hyd}}[(\text{SCN})_2])^2}{2[\text{SCN}^-][\text{H}^+][(\text{SCN}^-)[\text{H}^+] + K_{\text{hyd}}]} \quad (9)$$

From eq 9, it can be seen that the empirical rate law, eq 8, applies when *K*_{hyd} is much smaller than [SCN⁻][H⁺]. Thus, *k*_{dec} is identified as (3/2)*k*_{disp}*K*_{hyd}².

One conflicting report is as follows. In a pulse radiolysis study by Schöneshöfer et al., it was found that the decomposition is a first-order process at higher pH, contrary to the evidence at low pH.³² The same first step, SR5, was proposed, followed by the first-order decomposition of HOSCN. A value of 3.3 × 10⁻¹¹ M² was determined for *K*_{hyd}. If we use this value of *K*_{hyd}, the reported value of *k*_{dec} at low pH, and the relationship *k*_{dec} = (3/2)*k*_{disp}*K*_{hyd}², the resulting value of *k*_{disp} is 6 × 10¹⁷ M⁻¹ s⁻¹, which is impossibly large.

More conflicting evidence comes from a ¹³C NMR study of the formation of OSCN⁻ in the lactoperoxidase-catalyzed reaction of H₂O₂ with SCN⁻, where an intermediate is found that corresponds to no known species and is suggested to be NCS—O—SCN²⁻, formed through hydrolysis of (SCN)₂.³³ This paper also reports evidence for conversion of OSCN⁻ to

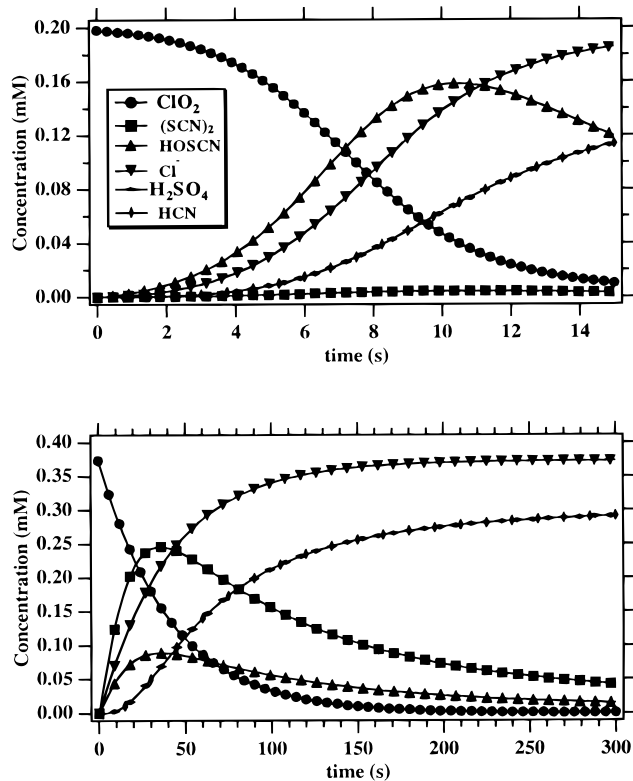


Figure 7. Simulation results for the mechanism in Table 2. Top: results for 0.01 M acid; $[\text{ClO}_2]_0 = 0.20$ mM, $[\text{SCN}^-]_0 = 25$ mM. Bottom: results for 1.0 M acid; $[\text{ClO}_2]_0 = 0.37$ mM, $[\text{SCN}^-]_0 = 25$ mM.

SCNO^- . It also calls into question data and inferences obtained in a widely cited ¹⁵N NMR study of the same reaction.³⁴

We conclude that the mechanism of hydrolysis of $(\text{SCN})_2$ at higher pH is unsettled, and thus the remainder of this paper is presented without further reference to it.

Success of the Model. Overall, it is clear that the mechanism in Table 2 accounts for the net stoichiometry given in reaction 2. Moreover, as described above, it leads to the observed pseudo-first-order rate law for loss of ClO_2 at low pH (eq 5).

Further evidence for its success is provided by the results of numerical integration of the system of differential equations arising from this mechanism. These simulations were performed with the Bulirsch–Stoer stiff integration routine available in the Specfit software package, and made use of the reactions given in Table 2 and the associated rate constants. The results, shown in Figure 7, qualitatively show the pseudo-first-order loss of ClO_2 in 1 M H^+ and the autocatalytic loss at pH 2. Quantitative agreement between these simulations and the observed kinetics is demonstrated by the excellent overlap of the traces shown in Figure 8 (pH 2) and Figure 9 (1 M H^+). The simulations accurately reproduce the first-order dependence on $[\text{SCN}^-]$ observed in 1 M H^+ . The simulation for 1 M H^+ also shows accumulation and loss of $(\text{SCN})_2$ in 1 M H^+ that is comparable to the properties of the intermediate revealed by EFA analysis. Finally, fitting of the model to the observed spectral traces in 1 M H^+ by treating the spectra of ClO_2 , $(\text{SCN})_2$, and products as variables led to the spectra in Figure 10; the spectra obtained for ClO_2 and products are entirely consistent with expectations for these species and require no further comment, while the spectrum derived for $(\text{SCN})_2$ is the first reported for this species in aqueous solution and is discussed further below.

Qualitatively, the inhibitory effects of the scavengers can be understood, since they should intercept SCN^- formed in steps

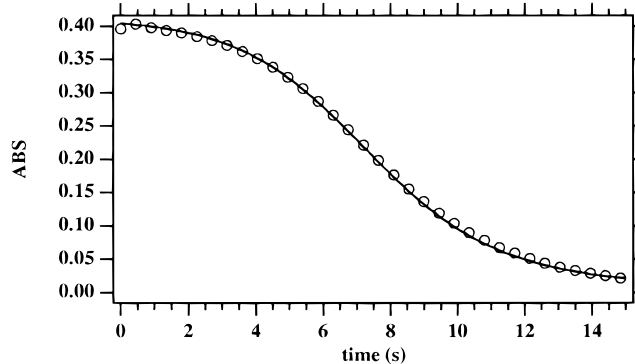


Figure 8. Comparison between computer simulations and experimental data for $\text{ClO}_2/\text{SCN}^-$ reaction at pH 2.0. The open circles represent raw data points and the solid line represents the simulation. The experimental data at 360 nm were extracted from multiwavelength data taken on the RSM 1000 at 25 °C in 0.01 M HClO_4 ; $[\text{ClO}_2]_0 = 0.20$ mM, $[\text{SCN}^-]_0 = 25$ mM.

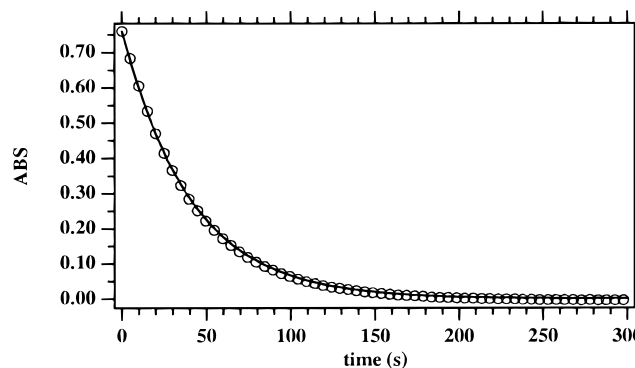


Figure 9. Comparison between computer simulations and experimental data for $\text{ClO}_2/\text{SCN}^-$ reaction at pH 0.0. The open circles represent raw data points, and the solid line represents the simulation. The experimental data at 360 nm were extracted from multiwavelength data taken on the RSM 1000 at 25 °C in 1.0 M HClO_4 ; $[\text{ClO}_2]_0 = 0.37$ mM, $[\text{SCN}^-]_0 = 25$ mM.

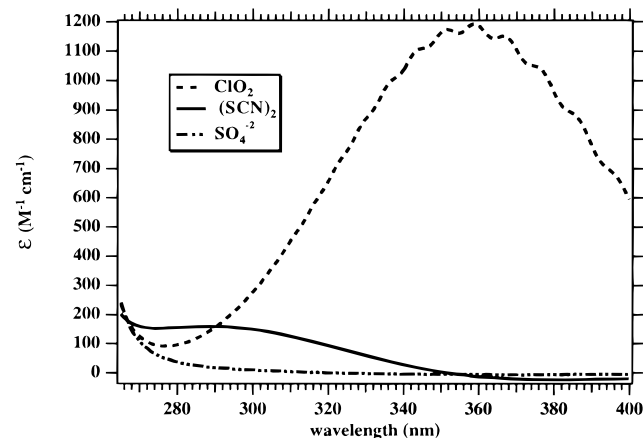


Figure 10. Spectra generated by a three-spectrum fit of the mechanism with rate constants as given in Table 2 to the data set shown in Figure 6 (unsparsed data used in the fit). The multiwavelength kinetic data were taken on the RSM 1000 at 25 °C in 1 M HClO_4 ; $[\text{ClO}_2]_0 = 0.37$ mM, $[\text{SCN}^-]_0 = 25$ mM.

SR1 and SR2 and $(\text{SCN})_2^-$ formed in step SR3, and they may also intercept OSCN^- formed in step SR10; the net effect should be a major reduction in the concentration of OSCN^- and a slowing of the consumption of ClO_2 via step SR10. Additional confirmation of the model comes through analysis of the rate constants in steps SR1 and (SR5 + SR13) as described below.

Overall, it is impossible to make a direct numerical comparison of the predictions of our model with that of Chinake et al.³ The problem is that the mechanism and rate constants provided in that work fail to yield the simulations reported in that work. As we have noted elsewhere,⁸ this appears to be a consequence of some typographical error.

Details of the Mechanism. Direct Reaction of ClO₂ and SCN⁻, SR1–SR2. The initial steps of the reaction of ClO₂ and SCN⁻ are accounted for in the one-electron transfers depicted in SR1 and SR2. SR1 is the simple one-electron reduction of ClO₂ to ClO₂⁻ and the formation of a thiocyanate radical. This type of reduction of ClO₂ is commonly invoked and well documented.^{3,35,36} Likewise, one-electron oxidation of SCN⁻ is commonly observed.²¹ SR2 is essentially a process equivalent to SR1, but is included to account for the acid dependence and two-term rate law derived experimentally. This step, which is the acid-catalyzed analogue of the first step, has no clear precedent in ClO₂ chemistry. Indeed, the kinetics of ClO₂ reactions are not generally reported for strongly acidic conditions where this second step becomes significant. Detailed analysis of this step would necessarily entail the protonation of SCN⁻, which occurs at high acid concentrations.³⁷ Although the pK_a of thiocyanic acid is unknown in 1 M ionic strength, at ionic strengths of 0.0, 2.0, and 4.0 M it has values of -1.1, -0.9, and -0.8, respectively.³⁸ Thus, under the conditions in the present work, the concentration of free SCN⁻ is not significantly altered through the formation of its conjugate acid. The values of *k*₁ and *k*₂ given in Table 2 are those obtained experimentally from rate law 5.

Reaction SR1 is the most important step in the mechanism, since it is one of the two rate-limiting steps in 1 M acid and it is the initiation step for the chain reaction at pH 2. This step is the simple bimolecular one-electron transfer oxidation of SCN⁻ by ClO₂; it is assigned a rate constant of 0.21 M⁻¹ s⁻¹, obtained by the fit to eq 4. A crucial test of this rate constant is that its microscopic reverse (*k*₋₁, the reduction of SCN by ClO₂⁻) must have a rate constant that does not exceed the diffusion-controlled limit. A value for *k*₋₁ can be calculated from the principle of detailed balancing as *k*₁/*K*₁, where *K*₁ can be calculated from the reduction potentials for the ClO₂/ClO₂⁻ and SCN/SCN⁻ redox couples. For the ClO₂/ClO₂⁻ couple, *E*^o is determined unambiguously as 0.934 V by its reversible electrochemistry.³⁹ The SCN/SCN⁻ couple is not as definitively established, but a number of lines of evidence support a value of 1.61 V for this reduction potential.⁴⁰ These *E*^o values yield *K*₁ = 3.7 × 10⁻¹², and combined with our result for *k*₁ yield a value of 5 × 10¹⁰ M⁻¹ s⁻¹ for *k*₋₁. In view of the effect that the high ionic strength of our experiments could have upon the value of *K*₁, our calculated result for *k*₋₁ appears to lie right at the diffusion-controlled limit. The high value of 201 M⁻¹ s⁻¹ previously reported³ for *k*₁ requires a value for *k*₋₁ that exceeds the diffusion-controlled limit by a factor of 5000, clearly an unacceptable result. Current thinking about one-electron oxidations of SCN⁻ states that rate constants such as *k*₁ should adhere rather rigorously to a LFER with unit slope when log *k* is plotted as a function of log *K*.^{21,22} The basis for this LFER, which was obtained from reactions of SCN⁻ with substitution-inert coordination complexes, is that back electron transfer (the reverse of SR1) is generally diffusion controlled for reactions involving the SCN/SCN⁻ redox couple. Apparently, this generalization also applies to the reaction with ClO₂ as the oxidant.

Fate of SCN, SR3. The near-diffusion-controlled reaction of SCN with SCN⁻ to form (SCN)₂⁻ is well established, and the literature value is used in Table 2.⁴¹ Under the conditions of

our experiments, with a large excess of SCN⁻, reaction SR3 is the most likely process for SCN to undergo. Dimerization of SCN, the decay path for SCN suggested by Chinake et al.,³ can be rejected, since the low steady-state concentrations of SCN would extensively favor reaction with SCN⁻ as in SR3.

Fate of (SCN)₂⁻, SR4. The radical (SCN)₂⁻ is proposed to be oxidized rapidly to (SCN)₂ by ClO₂. Although we have no direct evidence for this step, it is proposed in analogy to other reactions of SCN⁻ with one-electron oxidants.²¹ Such a pathway has been directly observed in a pulse radiolysis study of the reaction of (SCN)₂⁻ with [Os(bpy)₃]³⁺.⁴² The value of the rate constant used in Table 2 has been selected arbitrarily at the diffusion limit, although values considerably smaller should have no significant effect on the results of the simulations.

Acid/Base Equilibria for HClO₂ and HOSCN, SR6–SR7. The equilibria represented by SR6 and SR7 are based on the standard *K*_a values for the systems (p*K*_a = 5.3 for HOSCN, p*K*_a = 1.72 for HClO₂).^{30,38} The protonations are assumed to be diffusion controlled and the dissociations are calculated accordingly. Oddly, a value of 3.1 × 10⁻⁶ M for the *K*_a of HClO₂ is implied by the rate constants used in the prior study by Chinake et al.³ This value is in complete disagreement the well-established literature value (1.9 × 10⁻² M)³⁸ and must be rejected.

Fate of HClO₂ and HOCl, SR8–SR9. These two steps provide an additional means for the formation of thiocyanogen, as HOSCN will be converted to it through SR5 under the right conditions. The rate constant for SR8 (HClO₂ + SCN⁻) is an estimate obtained by adjustment for a good fit of the simulations to the observed kinetic data; the value of 180 M⁻¹ s⁻¹ fits the data well. In analogy with other reactions of HOCl,⁴³ step SR9 (HOCl + SCN⁻) likely proceeds via ClSCN, which then hydrolyzes to HOSCN. A reasonable estimate for *k*_{SR9} can be made by use of the well-established Swain–Scott relationship for reactions of HOCl with nucleophiles.⁴³ Interpolation of the published Swain–Scott plot with the nucleophilicity parameter⁴⁴ *n* of 4.77 for SCN⁻ yields a value of about 10⁷ M⁻¹ s⁻¹ for *k*_{SR9}. In fact, the simulations are highly insensitive to the actual value used, and values as low as 1 × 10³ M⁻¹ s⁻¹ yield essentially identical results. Our value for *k*_{SR9} is approximately 2 × 10⁶ times larger than that used previously;³ however, it remains unclear as to the units of that reported rate constant such that the magnitude of this difference remains in doubt.

Hydrolysis of (SCN)₂, SR5. The equilibrium represented by SR5, *K*_{hyd}, is perhaps the most critical step in these simulations. It is widely believed to be the first step in the hydrolysis of (SCN)₂. The rate constants used were obtained by adjustment so as to obtain good agreement between the simulations and the experimental data. It should be noted that the equilibrium constant implied by these rate constants (*K*_{hyd} = 8.8 × 10⁻³ M²) deviates by several orders of magnitude from the pulse radiolysis value reported by Schöneshöfer et al.,³² but this disagreement is disregarded for reasons discussed above. Considerably better agreement is found with the value of 2 × 10⁻⁵ M² obtained from an analysis of the complex kinetics of the reaction of acidic SCN⁻ with BrO₃⁻;⁴⁵ closer agreement would be unexpected in view of the uncertainties involved.

Oxidation of OSCN⁻ by ClO₂, SR10 and SR11. These steps are essential in providing an additional pathway for the consumption of ClO₂ that can become active at higher pH and generate the observed autocatalytic behavior. Step SR10 is a simple one-electron oxidation of OSCN⁻ by ClO₂ and is analogous to the oxidation of SCN⁻ by ClO₂. As there are no prior reports of the one-electron oxidation of OSCN⁻, the rate constant used is just that required to obtain a good fit to the

data. Step SR11 indicates the disproportionation of the OSCN radical as a second-order process and is analogous to the disproportionation of OBr.⁴⁶ Most likely the reaction proceeds via dimerization and subsequent hydrolysis. The rate constant used is arbitrary and selected to be fast. Since the species OSCN has not been reported previously and has only hypothetical existence, alternative loss pathways could occur, as in SR3 for SCN.

Steps SR10 and SR11 represent the largest conceptual departure of this mechanism from that suggested by Chinake et al.³ These prior workers suggested the reaction of ClO₂ with Cl⁻ to form HClO₂ plus HOCl as the additional pathway for loss of ClO₂, instead of the reaction with OSCN⁻ that we propose. The basis for this change of mechanism is our belief that ClO₂ does not react with Cl⁻ rapidly enough to contribute significantly in the ClO₂/SCN⁻ reaction. Details of this view are sufficiently complex to require a separate publication for exposition.⁸

Thiocyanogen Decomposition, SR5,12–14. It is widely accepted in the literature, that thiocyanogen hydrolyzes via a series of rapid steps, the first of which is SR5.^{34,47,48} The subsequent steps are represented in this mechanism by SR12 through SR14. This type of pathway has been proposed since the early part of this century.²⁸ We have elected to omit the reaction HOSCN + HO₂SCN → HO₃SCN + SCN⁻ + H⁺, since there is no published evidence for its participation in the hydrolysis of (SCN)₂ and since we find that it has no effect on the simulated decay of (SCN)₂ even for rate constants as large as 1 × 10⁶ M⁻¹ s⁻¹. An alternative mode for decomposition of (SCN)₂ has been suggested to involve steps SR5 and SR13 to form HO₂SCN, followed by acid hydrolysis of HO₂SCN to form H₂SO₃ plus HCN.^{45,49,50} Further oxidation of H₂SO₃ to SO₄²⁻ could occur through reaction with ClO₂, (SCN)₂, or other oxidants present in solution. We are not able to rule out this possibility and hence our choice of mechanism is somewhat arbitrary.

The simulations were found to be very sensitive to the value selected for *k*_{disp} (SR13), and the value used is that required for optimal fits. The simulations are not sensitive to the rate constants used for SR12 and SR14, and so the values used are arbitrarily selected to be fast. From the relationship *k*_{dec} = (3/2)*k*_{disp}*K*_{hyd}², the rate constants in Table 2 yield a value of 9 × 10⁻² M³ s⁻¹ for *k*_{dec}. This result is 90-fold greater than that measured by Stedman and Whincup at 0 °C,²⁹ and thus suggests a considerable thermal coefficient for *k*_{dec}. Our values for *k*_{disp} and for SR12 differ substantially from those used by Chinake et al.,³ but these differences are not unexpected in view of the overall difference between the two mechanisms. Zhang and Field used a value of 1 × 10⁹ M⁻¹ s⁻¹ for *k*_{disp} in their study of the BrO₃⁻/SCN⁻ reaction.⁴⁵ While this value differs by several orders of magnitude from ours, it is unclear whether a rate constant similar to ours (with a compensating change in *K*_{hyd}) could have been used in that study.

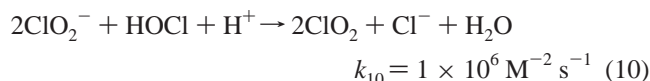
(SCN)₂ UV Spectrum. The spectrum of (SCN)₂ derived by kinetic fitting is shown in Figure 10 and is the first reported for this species in aqueous solution. It is characterized by λ_{max} = 288 nm and ε₂₈₈ = 159 M⁻¹ cm⁻¹ and shows good agreement with the derived broad-band absorbance associated with the intermediate by EFA (λ_{max} around 275 nm). (SCN)₂ is stable in CCl₄, and its UV-vis spectrum has long been known (λ_{max} at 295 nm and ε = 140 M⁻¹ cm⁻¹).²⁷ The implied solventochromism of (SCN)₂ bears comparison with that for iodine. Aqueous iodine solutions are known to show variability in molar absorptivity and λ_{max} as a function of acid strength and composition.⁵¹ Significant shifts also occur in organic solvents,

as shown by the values of λ_{max} in C₇H₁₆ (520 nm) and acetone (363 nm).⁵² Notable also is the shift for iodine in CCl₄ (540 nm) to water (470 nm), corresponding to an energy change of 2.8 × 10³ cm⁻¹.⁵³ This shift is similar to the shift that we obtain for thiocyanogen, 2.5 × 10³ cm⁻¹. The molar absorptivity of I₂ as a function of solvent varies up to 30%, and our derived molar absorptivity for aqueous (SCN)₂ falls within the same range as that reported for CCl₄ solutions.

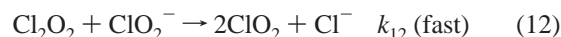
A literature report on the UV spectrum of aqueous (SCN)₂ can be found in the Ph.D. thesis of Long, as cited by Dolbear and Taube (λ_{max} = 302 nm and ε₃₀₂ = 840 M⁻¹ cm⁻¹).⁵⁴ While Long's value of ε₃₀₂ disagrees with the value to be expected from the spectrum in CCl₄, the value of λ_{max} is not that far off.

In spectroelectrochemical studies of the oxidation of SCN⁻, it was reported that the strongly absorbing species (SCN)₃⁻ rather than (SCN)₂ is generated.^{55,56} This inference was based on the drastic differences between the spectrum of the observed intermediate and that reported for (SCN)₂. A gold minigrad electrode was used in these studies; most likely the observed species was a gold-thiocyanate complex, formed through electrodisolution of the electrode. At present there is no compelling evidence that (SCN)₃⁻ forms to a significant degree in aqueous solution.

ClO₂ Formation. An additional step is required in order to explain the production of ClO₂ and the oligooscillatory behavior in the reaction of ClO₂⁻ with thiocyanate noted in previous work.^{3,4} The most likely candidate is



This reaction has been studied extensively^{5,57} and although its inclusion in our mechanism had no discernible effect on the results of the simulations and fits, it should become significant at high concentrations of ClO₂⁻. This step, as noted in the literature,^{3,5,57} is probably a two-step process and can be represented by the following:



With the second step being fast, this sequence leads to a first-order dependence on chlorite. The general model rate constants presented by Rábai and Orbán⁵ for these steps are consistent with this description.

Conclusions

The results described above modify or add to prior observations on the SCN⁻/ClO₂ reaction in the following significant ways. (1) The stoichiometry of the reaction is now believed to entail formation of HCN rather than OCN⁻. (2) The kinetics have been shown to become pseudo-first-order in strongly acidic media. (3) The rate law for noncatalytic reaction of ClO₂ with SCN⁻ has now been determined, affording a direct measurement of the rate constant for electron transfer from SCN⁻ to ClO₂ that is a factor of 1000 smaller than previously believed. This new rate constant is consistent with the demands of detailed balancing and the rule that spontaneous one-electron reductions of the SCN radical are diffusion controlled. (4) Formation of an intermediate absorbing in the UV has been observed and identified as (SCN)₂, which places major constraints on models of the reactive system.

These results have required major alterations to the prior reaction model. Further significant alterations include the use of the correct pK_a for HClO₂, the rejection of the reaction of Cl⁻ with ClO₂, and the inclusion of the reaction of OSCN⁻ with ClO₂. It is this latter reaction that leads to autocatalytic consumption of ClO₂ in the model. Although considerable uncertainty remains regarding certain features of the mechanism, particularly with respect to the details of the decomposition of (SCN)₂, overall the model is consistent with the observed results and is a major improvement over the prior model.

Acknowledgment. This research was supported by a grant from the NSF. Dr. R. Binstead is thanked for his assistance in the development and use of Specfit, Prof. E. Bakker (Auburn University) is thanked for his advice concerning the use of ion-specific electrodes, and Prof G. Stedman (University of Wales Swansea) is thanked for his comments regarding thiocyanogen chemistry. Professor Fred Anson (Caltech) is thanked for graciously acting as a sabbatical host to D.M.S. during the preparation of this manuscript.

Supporting Information Available: Figure 1S, showing k_{obs} vs [SCN⁻]. Figure 2S, showing k_{obs} vs [H⁺]. Figure 3S, showing the temperature dependence of k_{obs} . This material is available free of charge via the Internet at <http://pubs.acs.org>.

References and Notes

- Alamgir, M.; Epstein, I. R. *J. Phys. Chem.* **1985**, *89*, 3611–3614.
- Doona, C. J.; Doumbouya, S. I. *J. Phys. Chem.* **1994**, *98*, 513–517.
- Chinake, C. R.; Mambo, E.; Simoyi, R. H. *J. Phys. Chem.* **1994**, *98*, 2908–2916.
- Doona, C. J. *J. Phys. Chem.* **1995**, *99*, 17059–17060.
- Rábai, G.; Orbán, M. *J. Phys. Chem.* **1993**, *97*, 5935–5939.
- Lengyel, I.; Rábai, G.; Epstein, I. R. *J. Am. Chem. Soc.* **1990**, *112*, 9104–9110.
- Epstein, I. R.; Kustin, K. *J. Phys. Chem.* **1985**, *89*, 2275–2282.
- Stanbury, D. M.; Figlar, J. N. *Coord. Chem. Rev.*, in press.
- Lednický, L. A.; Stanbury, D. M. *J. Am. Chem. Soc.* **1983**, *105*, 3098–3101.
- Masschelein, W. J. *Chlorine Dioxide*; Ann Arbor Science: Ann Arbor, 1979; p 190.
- Morf, W. E. *The Principles of Ion-Selective Electrodes and of Membrane Transport*; Elsevier Scientific Publishing Co.: New York, 1981; pp 1–433.
- Ionophores, Membranes, Mini-ISE*; Fluka Chemical Corp.: Ronkonkoma, NY, 1996; pp 56–57.
- Binstead, R. A.; Zuberbühler, A. D. *SPECFIT*; Spectrum Software Associates: Chapel Hill, 1995.
- Doona, C. J.; Blittersdorf, R.; Schneider, F. W. *J. Phys. Chem.* **1993**, *97*, 7258–7263.
- Epstein, I. R.; Kustin, K.; Simoyi, R. H. *J. Phys. Chem.* **1992**, *96*, 5852–5836.
- Dodgen, H.; Taube, H. *J. Am. Chem. Soc.* **1949**, *71*, 2501–2504.
- Taube, H.; Dodgen, H. *J. Am. Chem. Soc.* **1949**, *71*, 3330–3336.
- Bray, W. Z. *Phys. Chem. (Leipzig)* **1906**, *54*, 569–608.
- Doona, C. J.; Stanbury, D. M. *Inorg. Chem.* **1996**, *35*, 3210–3216.
- Moore, R. H.; Zeigler, R. K. *LSTSQ*; Los Alamos National Laboratory: Los Alamos, NM, 1959.
- Hung, M.-L.; Stanbury, D. M. *Inorg. Chem.* **1994**, *33*, 4062–4069.
- Nord, G. *Comments Inorg. Chem.* **1992**, *13*, 221–239.
- Gampp, H.; Maeder, M.; Meyer, C. J.; Zuberbühler, A. D. *Talanta* **1985**, *32*, 95–101.
- Gampp, H.; Maeder, M.; Meyer, C. J.; Zuberbühler, A. D. *Talanta* **1985**, *32*, 257–264.
- Gampp, H.; Maeder, M.; Meyer, C. J.; Zuberbühler, A. D. *Talanta* **1985**, *32*, 1133–1139.
- Gampp, H.; Maeder, M.; Meyer, C. J.; Zuberbühler, A. D. *Talanta* **1986**, *33*, 943–951.
- Schöneshöfer, M.; Irwin, R. S. *J. Chem. Soc.* **1958**, 778–784.
- Bjerrum, N.; Kirschner, A. *Chem. Abstr.* **1919**, *13*, 1057–1060.
- Stedman, G.; Whincup, P. A. E. *J. Chem. Soc. A* **1969**, 1145–1148.
- Thomas, E. L. *Biochemistry* **1981**, *20*, 3273–3280.
- Kornath, A.; Blecher, O.; Ludwig, R. *J. Am. Chem. Soc.* **1999**, *121*, 4019–4022.
- Schöneshöfer, M.; Beck, G.; Henglein, A. *Ber. Bunsen-Ges. Phys. Chem.* **1970**, *74*, 1011–1015.
- Pollock, J. R.; Goff, H. M. *Biochim. Biophys. Acta* **1992**, *1159*, 279–285.
- Modi, S.; Deodhar, S. S.; Behere, D. V.; Mitra, S. *Biochemistry* **1991**, *30*, 118–124.
- Stanbury, D. M.; Martinez, R.; Tseng, E.; Miller, C. E. *Inorg. Chem.* **1988**, *27*, 4277–4280.
- Awad, H. H.; Stanbury, D. M. *J. Am. Chem. Soc.* **1993**, *115*, 3636–3642.
- Jones, E.; Munkley, C. G.; Phillips, E. D.; Stedman, G. *J. Chem. Soc., Dalton Trans.* **1996**, 1915–1920.
- Smith, R. M.; Martell, A. E.; Motekaitis, R. J. *NIST Critically Selected Stability Constants of Metal Complexes Database*, 2.0; U.S. Department of Commerce: Gaithersburg, MD, 1995.
- Stanbury, D. M. *Adv. Inorg. Chem.* **1989**, *33*, 69–138.
- Sarala, R.; Rabin, S. B.; Stanbury, D. M. *Inorg. Chem.* **1991**, *30*, 3999–4007.
- Neta, P.; Huie, R. E.; Ross, A. B. *J. Phys. Chem. Ref. Data* **1988**, *17*, 1027–1284.
- Nord, G.; Pedersen, B.; Floryan-Løvborg, E.; Pagsberg, P. *Inorg. Chem.* **1982**, *21*, 2327–2330.
- Gerritsen, C. M.; Margerum, D. W. *Inorg. Chem.* **1990**, *29*, 2757–2762.
- Swain, C. G.; Scott, C. B. *J. Am. Chem. Soc.* **1953**, *75*, 141–147.
- Zhang, Y.-X.; Field, R. J. *J. Phys. Chem.* **1992**, *96*, 1224–1228.
- Kläning, U. K.; Wolff, T. *Ber. Bunsen-Ges. Phys. Chem.* **1985**, *89*, 243–245.
- Aune, T. M.; Thomas, E. L. *Eur. J. Biochem.* **1977**, *80*, 209–214.
- Hughes, M. N. In *Chemistry and Biochemistry of Thiocyanic Acid and its Derivatives*; Newman, A. A., Ed.; Academic Press: New York, 1975; pp 2–67.
- Wilson, I. R.; Harris, G. M. *J. Am. Chem. Soc.* **1961**, *83*, 286–289.
- Smith, R. H.; Wilson, I. R. *Aust. J. Chem.* **1967**, *20*, 1353–1366.
- Buckles, R. E.; Mills, J. F. *J. Am. Chem. Soc.* **1953**, *75*, 552–555.
- Benesi, H. A.; Hildebrand, J. H. *J. Am. Chem. Soc.* **1949**, *71*, 2703–2707.
- Kleinberg, J.; Davidson, A. W. *Chem. Rev.* **1948**, *42*, 601–609.
- Dolbear, G. E.; Taube, H. *Inorg. Chem.* **1967**, *6*, 60–64. See also the similar spectral data reported in ref 29.
- Itabashi, E. *J. Electroanal. Chem.* **1984**, *177*, 311–315.
- Itabashi, E. *Inorg. Chem.* **1985**, *24*, 4024–4027.
- Peintler, G.; Nagypál, I.; Epstein, I. R. *J. Phys. Chem.* **1990**, *94*, 2954–2958.